CHAPTER IV
RESULTS AND DISCUSSION

4.1 Adsorbent Characterizations

4.1.1 Morphology of Activated Carbon Surface Observed by SEM

In this study, activated carbon from Norit, Calgon, and activated carbon derived from coconut shell and from eucalyptus were used as an adsorbent. The morphologies of the samples were investigated by SEM as shown in Figures 4.1 to 4.5. There are three different pore structures observed on the activated sample surfaces; the large pore size, the small pore size and the sponge pore structure. At 2,000 magnifications, the relative large pore sizes in the range of 2.5-7.5μm can be clearly observed on the untreated activated carbon surfaces from Norit and from activated carbon derived from coconut shell (20-40 mesh). On the contrary, rough surfaces are observed from the other three untreated activated carbon from Calgon, from eucalyptus and from coconut shell (powder). At 5,000 magnifications, the smaller pore sizes of this pore type can be seen from all five activated carbon samples at 5,000 magnifications. Furthermore, there is another pore structure type observed on pore the Calgon sample at 10,000 magnifications in Figure 4.2 c). This pore structure resemble to sponge structure.

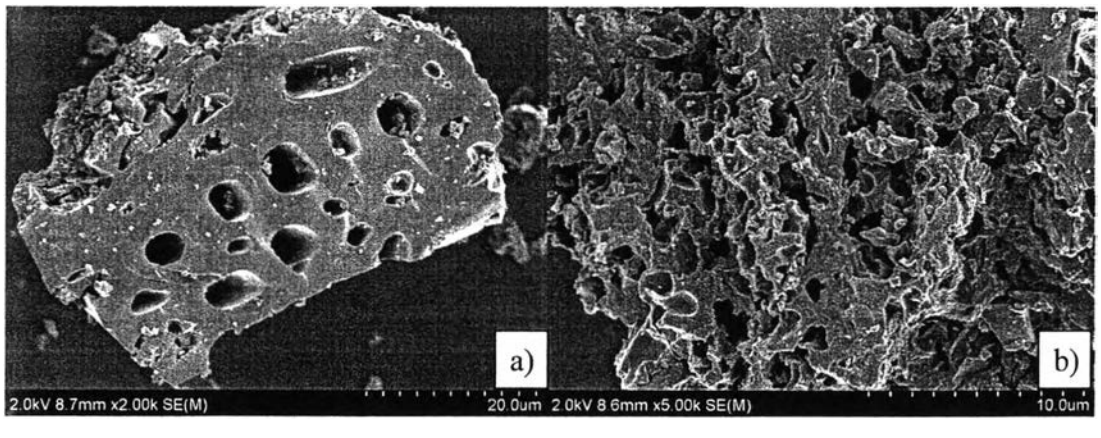

Figure 4.1 Micrographs of untreated activated carbon from Norit at a) 2,000 and b) 5,000 magnifications.

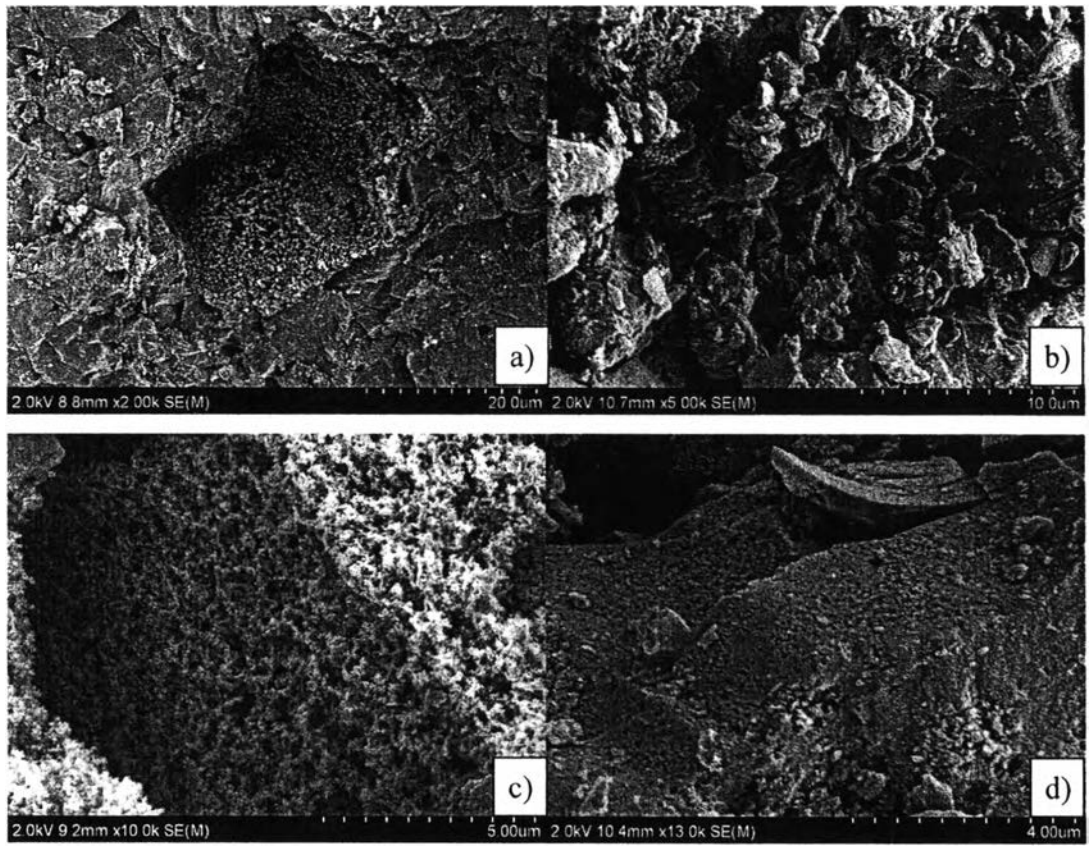

Figure 4.2 Micrographs of untreated activated carbon from Calgon at (a) 2,000 (b) 5,000 (c) 10,000 and (d) 13,000 magnifications.

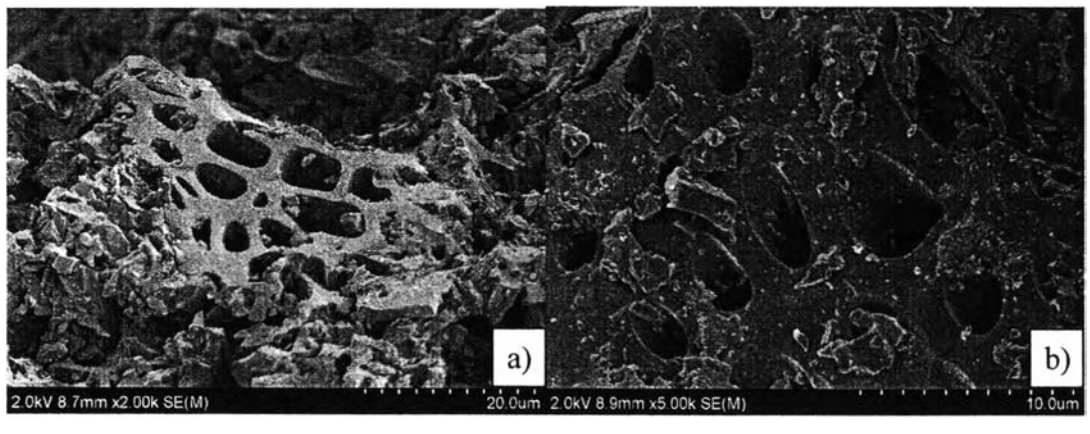

Figure 4.3 Micrographs of untreated activated carbon derived from coconut shell (20-40 mesh) at a) 2,000 and b) 5,000 magnifications.

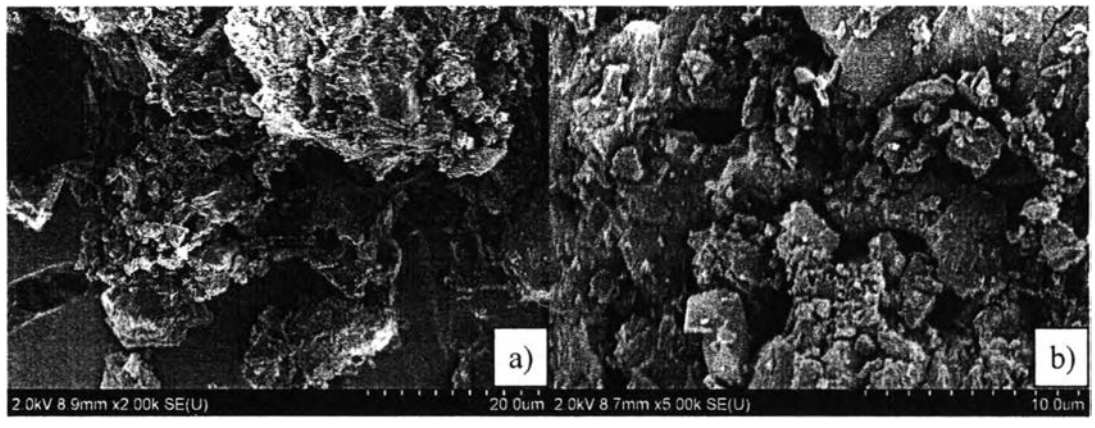

Figure 4.4 Micrographs of untreated activated carbon derived from coconut shell (powder) at a) 2,000 and b) 5,000 magnifications.

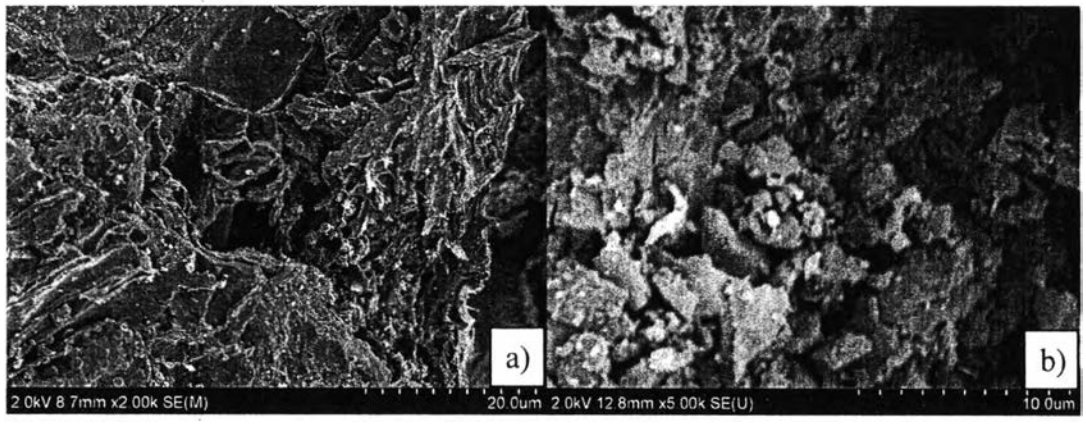

Figure 4.5 Micrographs of untreated activated carbon derived from eucalyptus at a) 2,000 and b) 5,000 magnifications.

In chemical treatment, all five carbon samples were treated with in acid (HCl, H_2SO_4 and HNO_3) or base (KOH) by soaking the carbon sample into solution to eliminate impurities on sample surface. After treatment, the effect of chemical treatment was investigated. The changing on morphology of treated activated carbon is then explored by using SEM. Figures 4.6 to 4.10 shows untreated and treated carbons surface morphology at 2,000 magnifications. At these magnifications, only the overall surface and macropores of the carbon sample can be observed. As a result, the morphology of each sample present different in effect of chemical treatment.

For the activated carbon from Norit, the untreated sample shows the macropore structure whereas the treated sample show blocking and collapsing of macropores on some area. In Figure 4.6b, the blocking of macropore structure morphology was found on KOH treated activated carbon. The blocking of macropore observed on activated carbon from Norit in KOH treatment may cause from the deposition of KOH molecule. This assumption shows the agreement with the study by Xiao *et al.* (2008). In their experiment, KOH can remain on pore wall and result in blocking of pore structure during treatment process. Figure 4.6d also show the blocking of macropore structure on the sample surface after HNO_3 treatment. Moreno-Castilla *et al.* (1997) defined that the oxygenated terminal groups can be produced and deposited on pore wall during HNO_3 treatment. Similar to KOH molecule in KOH treatment, the oxygenated terminal group deposition leads to blocking of adsorbent macropore structure. In Figure 4.6c and 4.6d, the collapsing of macropore can be observed on the sample surface after HCl and H_2SO_4 treatment. The possible mechanism to explain collapse of pore structure is the mechanical destruction due to the surface tension. As in previous experiment, Moreno-Castilla *et al.* (1997) the strong oxidizing solution like HCl, H_2SO_4 and HNO_3 can cause the pore structure destruction. The surface tension of solution make the destruction of activated carbon occurs.

For activated carbon from Calgon (Figure 4.7), the similar rough surface morphology as the untreated surface was observed on the treated sample. The similar morphology with the untreated of chemical treated activated carbon may have changing in pore structure. As mention before, the magnifications used in the experiment allow only overall and macropore to be observed and the changing in smaller pore structure cannot be explored.

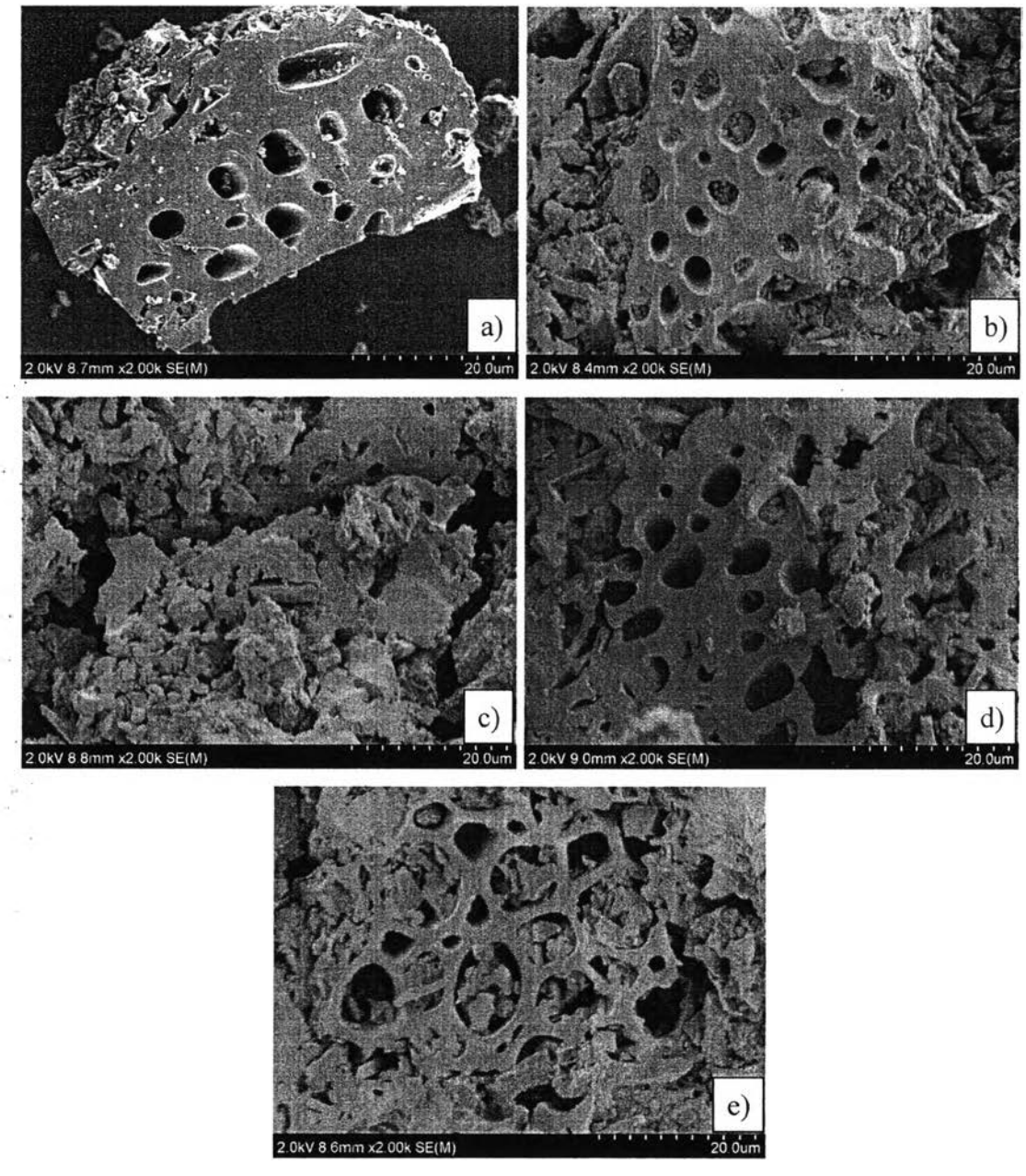

Figure 4.6 Micrographs of activated carbon from Norit a) untreated b) treated with KOH c) treated 1M HCl d) treated with 1M H_2SO_4 e) treated with HNO_3 at 2,000 magnifications.

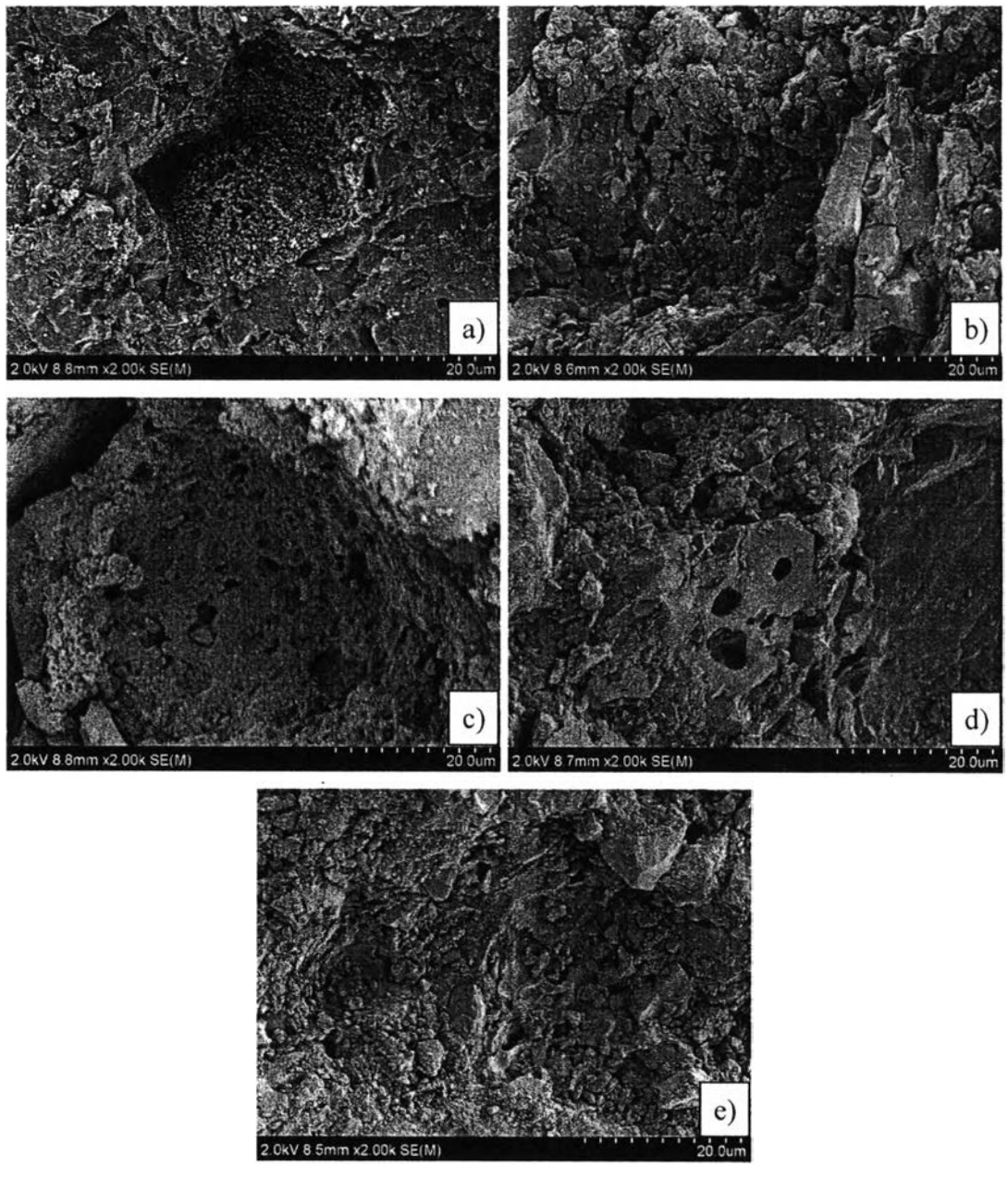

Figure 4.7 Micrographs of activated carbon derived from Calgon a) untreated b) treated with KOH c) treated 1M HCl d) treated with 1M H_2SO_4 e) treated with HNO_3 at 2,000 magnifications.

Different from activated carbon derived from coal sample, the activated carbons derived from coconut shell (20-40 mesh) show many types of surface morphology on both untreated and treated sample as shown in Figure 4.8. According to various elements content, coconut shell activated carbons show many types of surface after activation. Daud *et al.* (2004) investigate on pore development of activated carbon produced from palm shell and coconut shell. They found that the difference in lignin, hemicelluloses and cellulose content in palm shell and coconut shell have significantly effect on pore development and subsequently on pore structure. According to various types found on activated carbon surface, any conclusion cannot be drawn from SEM results.

Similar to activated carbon from Calgon, the rough surface morphology as the untreated surface can also be observed on the KOH and HNO_3 treated activated carbon from coconut shell (powder) sample surface in Figure 4.9b and 4.9d. In HCl and H_2SO_4 treatment, the carbon show small pore on surface as indicated in Figure 4.9c and 4.9e. Santiago *et al.* (2005) and Xiao *et al.* (2008) refer that treating activated carbon with oxidation agent like HCl, H_2SO_4 and HNO_3 can eliminate the impurities on the carbon surface.

For activated carbon that derived from eucalyptus, macropore structure can be observed on the surface after treating with chemical solution. For activated carbon derived from eucalyptus, the macropore structure can be found after acid treatment process and smaller pore structure can be found after base treatment. From Figure 4.10b-e, it can be clearly seen that treatment process resulted in a porous structure and the opening of pores on the surface of activated carbon. The appearance of small pore on surface may cause from the eliminating of impurities. The impurities would be dissolved in the solution, leading to the opening of plugged pores and enlarging of pre-existing pores during process.

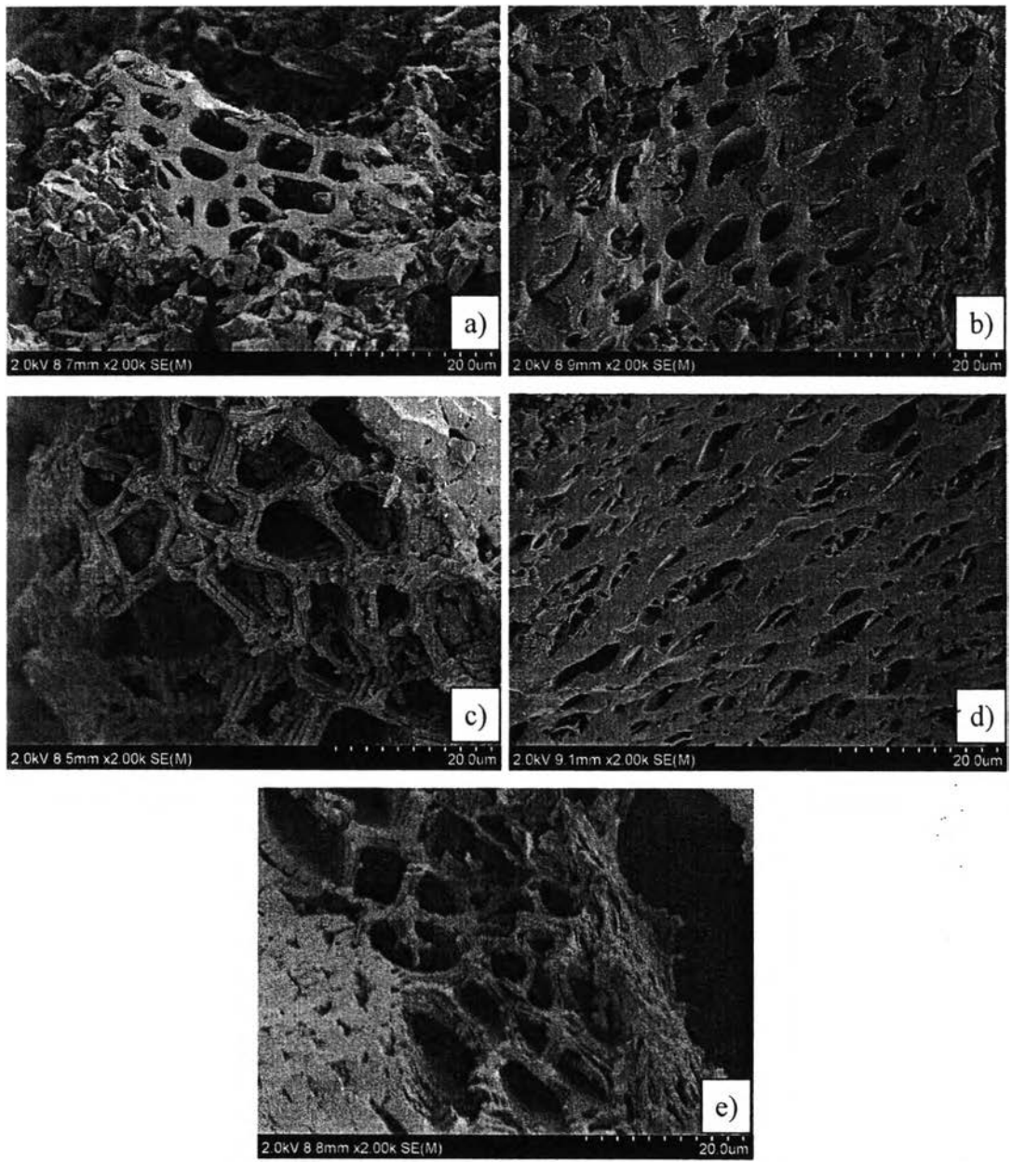

Figure 4.8 Micrographs of activated carbon derived from coconut shell (20-40mesh) a) untreated b) treated with KOH c) treated 1M HCl d) treated with 1M H_2SO_4 e) treated with HNO_3 at 2,000 magnifications.

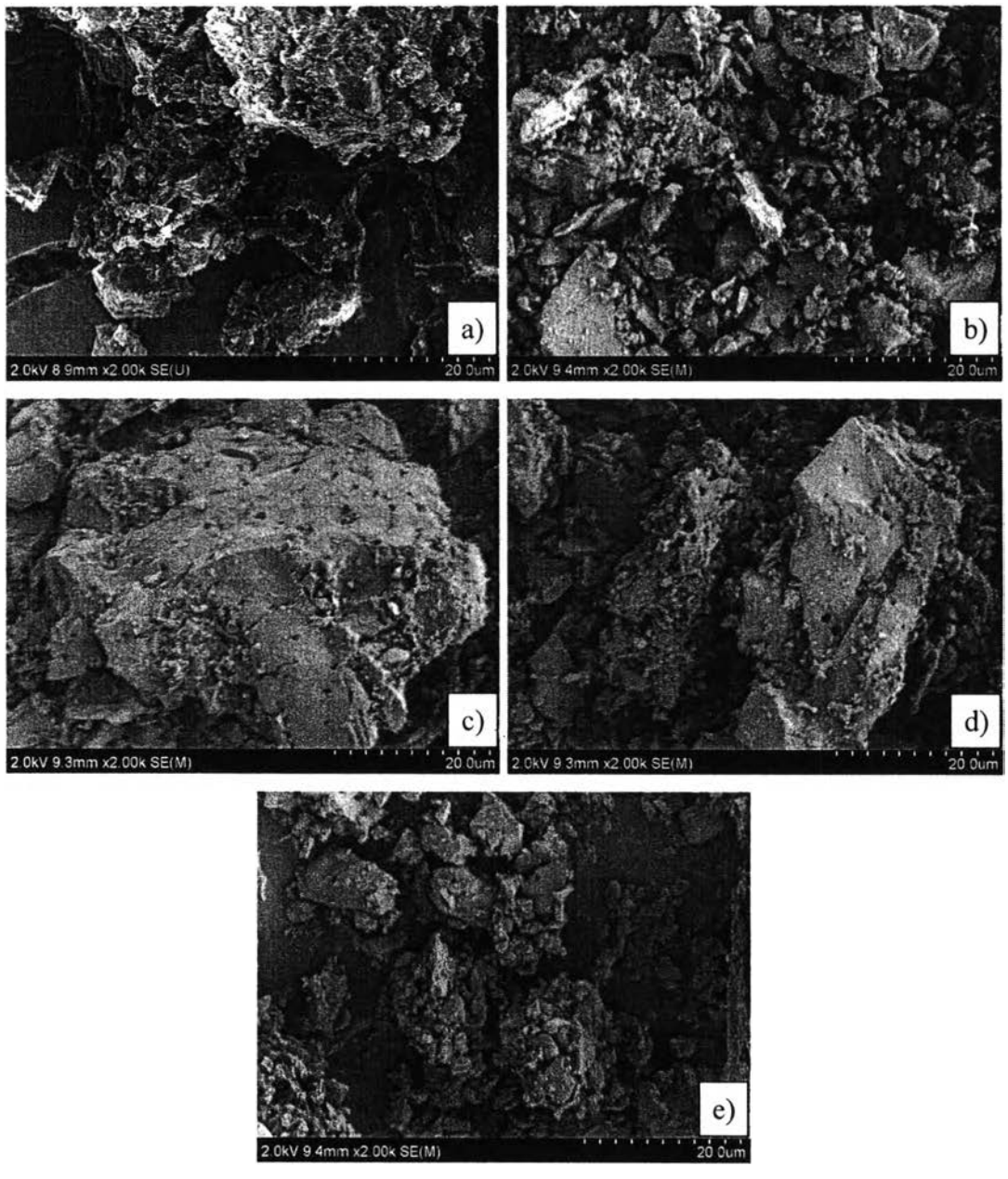

Figure 4.9 Micrographs of activated carbon derived from coconut shell (powder) a) untreated b) treated with KOH c) treated 1M HCl d) treated with 1M H_2SO_4 e) treated with HNO_3 at 2,000 magnifications.

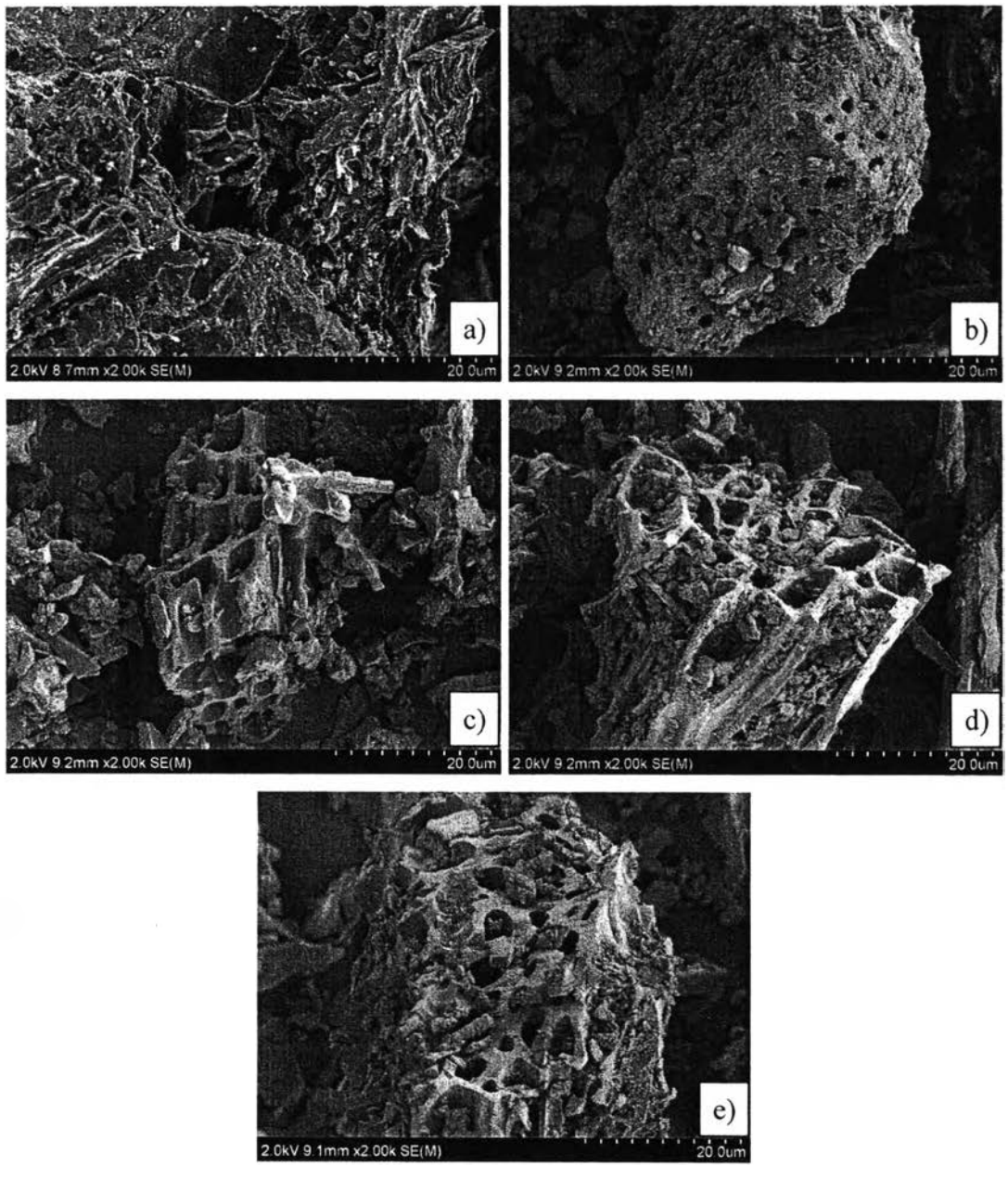

Figure 4.10 Micrographs of activated carbon derived from eucalyptus a) untreated b) treated with KOH c) treated 1M HCl d) treated with 1M H_2SO_4 e) treated with HNO_3 at 2,000 magnifications.

4.2.2 Surface Area Analysis of Activated Carbon

The surface area analysis of activated carbon sample was conducted using a nitrogen adsorption instruments at 77 K. Specific surface area, pore volume and average pore diameter are reported in Table 4.1. According to the International Union of Pure and Applied Chemistry (IUPAC), pores on activated carbons are classified by their sizes into three groups: macropores having an average diameter of greater than 50 nm, mesopores with a diameter of 2–50 nm, and micropores having an average diameter of less than 2 nm. Nitrogen adsorption isotherms of the activated carbon samples indicate that they contain mainly mesopores structure on their surface. According to the effect of activated carbon surface area and average pore diameter on methane adsorption capacity, the treated activated carbon physical surface properties were studied.

Table 4.1 to 4.5 indicates the sample physical surface properties of the activated carbon before and after chemical treatment. From surface area result, there is a significant decreasing of surface area observed from the chemical treated activated carbon from Norit as shown in Table 4.1. The activated carbon from Calgon surface area is also decreased in acid treatment but the surface area is increased in base treatment (Table 4.2). Other three natural source-based activated carbons; produced from coconut shell (20-40 mesh), coconut shell (powder) and eucalyptus; show the increasing of sample surface area after treatment.

Ahmadpour *et al.* (1998) studied the effect of carbon raw material type on activated carbon physical surface properties. In their experiment, the activated carbon from macadamia nutshell and from coal was treated with $ZnCl_2$ and KOH solution under the same condition. As a result, KOH treated macadamia nutshell shows the lowest surface area whereas the KOH treated coal shows the highest surface area comparing to other treated carbons. Due to volatile matters and ash content of their sample, the weight loss of carbon sample from macadamia nutshell was two times higher in $ZnCl_2$ and three times higher in KOH treatment than the sample from coal. So, they concluded that the type of porosity and pore size distribution in the carbon depends on the method of activation and the type of raw material. Similar to their experiment, the activated carbons from different source were used in this experiment; the coal-based commercial activated carbon from Norit

and Calgon; and the natural-based activated carbon from C Gigantic Carbon. According to the different in their structure, the activated carbons show different effect on surface area result.

After acid treatment process, the surface areas of activated carbon from Norit and Calgon are decreased. This result may be due to the collapse of pore structure. Moreno-Castilla *et al.* (1997) and Santiago *et al.* (2005) indicated that there is chlorine remaining on surface of activated carbon in HCl treatment process due to the complete ionic dissociation of HCl. The remaining chlorine reduces micropore volume and width of activated carbon micropore which led to decreasing of surface area. Furthermore, Moreno-Castilla *et al.* (1997) studied the effect of HNO_3 treatment and indicated that nitric acid can cause pore collapse. They defined two mechanisms to explain the breaking of the micropore walls after treatment with a strong oxidant such as HNO_3. Their explanation are 1) by oxidation to produce oxygenated terminal groups and 2) the mechanical destruction of the pores by the surface tension of the oxidizing solution.

On the other hand, the surface area of activated carbon derived from coconut shell and eucalyptus is increased after treated with acid. Santiago *et al.* (2005) indicated that the elimination of the inorganic elements in HCl treatment result in the increasing of activated carbon surface area. Xiao *et al.* (2008) also studied effect of H_2SO_4 and HNO_3 acid treatment. They refer that most of the impurities would be dissolved in the solution, leading to the opening of plugged pores and enlarging of pre-existing pores during process. Moreover, they refer that H^+ ions have significant effect to amount of impurities removed from sample. At the same concentration, H_2SO_4 can gives H^+ ions more than HNO_3, which can react with other more impurities, consequently resulting in the enhanced micropores volume.

For base treatment, Xiao *et al.* (2008) indicated that the decrease of surface area can be due to the deposition of KOH on pore wall, when the activated carbon was treated. The KOH deposition is difficult to be completely removed in the washing process. So, the deposition of KOH can cause the blocking of pore structure. Agree with their hypothesis, the surface area of base treated activated carbon from Norit is decreased by blocking of pore structure. On contrary, the surface areas of activated carbon from Calgon, from coconut shell and from eucalyptus are increased

in base treatment process. Sricharoenchaikul *et al.* (2007) refer that KOH can remove metal and impurities from crystallite of activated carbon structure. KOH can further create mesopore on the activated carbon surface.

Adsorbent average pore size is another important parameter for methane adsorption. Lozano-Castello *et al.* (2002) and Wang *et al.* (2011) indicated that the optimum pore size for methane storage applications is approximately 0.8 nm, which corresponds to a pore wall separation of about two methane molecules. If the pore size is considered as the distance between the middle of the carbon atoms at both walls, this distance is approximately 1.1 nm. The bigger pore size than the optimum, makes the methane adsorb with a lower density. The granular (20-40 mesh) activated carbon derived from coconut shell (Table 4.3) and the powder that derived from eucalyptus (Table 4.5) show agreement with this theory. The untreated activated carbon derived from coconut shell (20-40 mesh) which has a smaller average pore diameter than the untreated from eucalyptus, present a greater amount of methane adsorbed.

Table 4.1 Physical surface properties of activated carbon from Norit

No.	AC sample	BET surface area (m^2/g)	Total pore volume (cc/g)	Average pore diameter (Å)
1	Norit	1331.5	0.543	22.0
2	Norit-KOH	1015.8	0.564	22.2
3	Norit-1M HCl	828.2	0.491	22.7
4	Norit-1M H_2SO_4	929.5	0.521	22.4
5	Norit-HNO_3	795.3	0.487	23.1

Table 4.2 Physical surface properties of activated carbon from Calgon

No.	AC sample	BET surface area (m^2/g)	Total pore volume (cc/g)	Average pore diameter (Å)
1	Calgon	880.1	0.498	26.9
2	Calgon-KOH	902.2	0.557	24.7
3	Calgon-1M HCl	781.1	0.477	24.4
4	Calgon-1M H_2SO_4	829.1	0.510	24.6
5	Calgon-1M HNO_3	868.8	0.482	24.5

Table 4.3 Physical surface properties of activated carbon derived from coconut shell (20-40 mesh)

No.	AC sample	BET surface area (m^2/g)	Total pore volume (cc/g)	Average pore diameter (Å)
1	Coconut shell[a]	843.0	0.463	21.9
2	Coconut shell[a]-KOH	1013.0	0.567	22.4
3	Coconut shell[a]-1M HCl	953.2	0.531	22.3
4	Coconut shell[a]-1M H_2SO_4	915.4	0.497	22.7
5	Coconut shell[a]-1M HNO_3	944.0	0.548	21.8

[a] activated carbon-coconut shell from C Gigantic Carbon

Table 4.4 Physical surface properties of untreated activated carbon derived from coconut shell (powder)

No.	AC sample	BET surface area (m^2/g)	Total pore volume (cc/g)	Average pore diameter (Å)
1	Coconut shell (powder)[a]	698.1	0.495	28.3
2	Coconut shell (powder)[a]-KOH	783.4	0.479	28.6
3	Coconut shell (powder)[a]-1M HCl	745.4	0.448	28.8
4	Coconut shell (powder)[a]-1M H_2SO_4	740.1	0.446	24.1
5	Coconut shell (powder)[a]-1M HNO_3	885.1	0.624	28.2

[a] activated carbon-coconut shell from C Gigantic Carbon

Table 4.5 Physical surface properties of untreated activated carbon derived from eucalyptus

No.	AC sample	BET surface area (m^2/g)	Total pore volume (cc/g)	Average pore diameter (Å)
1	Eucalyptus[b]	861.0	0.607	28.2
2	Eucalyptus[b]-KOH	985.7	0.712	29.3
3	Eucalyptus[b]-1M HCl	917.2	0.644	28.1
4	Eucalyptus[b]-1M H_2SO_4	1005.0	0.725	28.8
5	Eucalyptus[b]-1M HNO_3	904.8	0.647	28.4

[b] activated carbon-eucalyptus from C Gigantic Carbon

4.2 Methane adsorption

4.2.1 Time Required to Reach Methane Adsorption Equilibrium

In adsorption isotherm experiment, methane adsoption capacity at each data points was measured and calculated at which the system reach the adsorption equilibrium. Therefore, time required to reach equilibrium need to be determined before performing the adsorption isotherm experiment. For determination required time, 700 psi pressure of methane was applied into reactor which contained 0.5g of activated carbon sample. After applying methane, the system was left for 3 hours. The data was collected from data logger and then were converted to amount of methane adsorbed using z-compressibility factor and mass balance basis. Figure 4.11 to 4.15 illustrate the amount of methane adsorbed versus time for the untreated and treated activated carbons. With almost the same total pore volume and average pore diameter of untreated and treated activated carbon, they require the same time for reaching the methane adsorption equilibrium. All of them achieve to methane adsorption equilibrium within 80 minutes. There is no significant effect on time require in chemical treatment. The only change which can apparently see is the methane adsorption capacity. Related with surface area result, the amount of methane adsorbed increase with the increasing of surface area.

Ahmadpour *et al.* (1998) inform that the high-energy micropore is interested for gas storage application because of their role in determining adsorption capacity. However, natural gas transportation to and from the micropores must also occur on a time scale short enough to make full use of the available capacity. In general, micropores are likely to display a long diffusional time scale. Mesopores and macropores are therefore required to provide rapid transport of gas through the particle coordinate. Compare to result from this experiment, rapid methane adsorption can be observed at the beginning and then the amount of methane adsorbed is gradually increased until the system reach the adsorption equilibrium. After opening the valve, adsorption of methane molecule on the mesopore structure firstly occur and next the methane molecule will diffuse and be adsorbed into a smaller pore. Chand *et al.* (2009) indicated that the surface modification produced carbon samples with a very different chemical nature but similar pore structure. The

only difference was a small decrease in the volume of the pores, which was also verified by the nitrogen adsorption–desorption isotherms, suggesting that the carbon materials maintain a microporous structure even after oxidation. The pore size distribution is almost the same before and after the oxidation. Related to this work, a small change in surface area and almost the same average pore diameter can be observed. There is no change both external diffusion and intraparticle diffusion after treatment due to only a small change in the average pore diameter

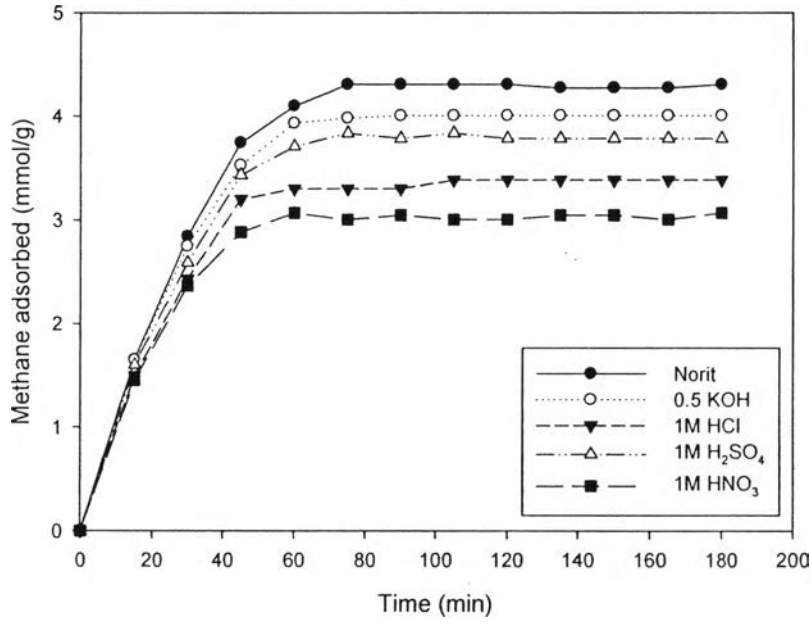

Figure 4.11 Methane uptake of activated carbons from Norit at 40°C temperature and 700 psi pressure.

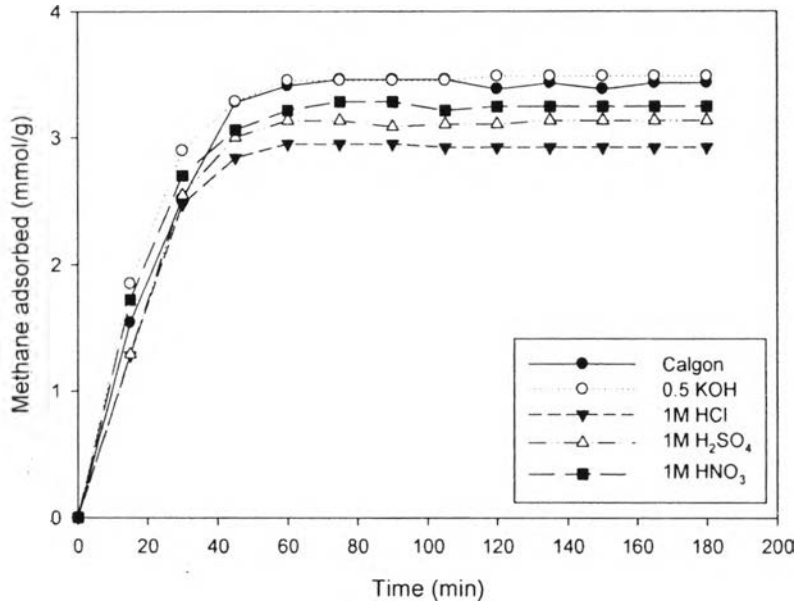

Figure 4.12 Methane uptake of activated carbons from Calgon at 40°C temperature and 700 psi pressure.

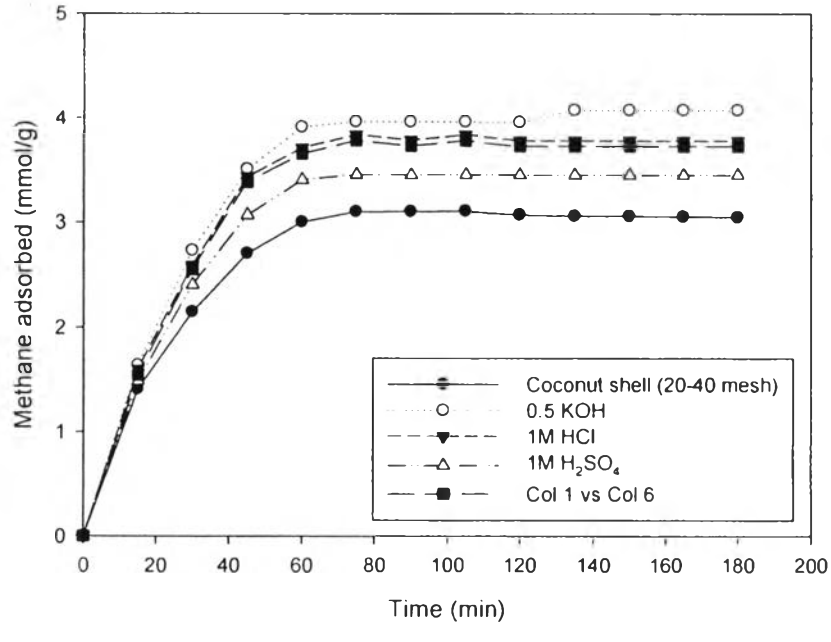

Figure 4.13 Methane uptake of activated carbons derived from coconut shell (20-40 mesh) at 40°C temperature and 700 psi pressure.

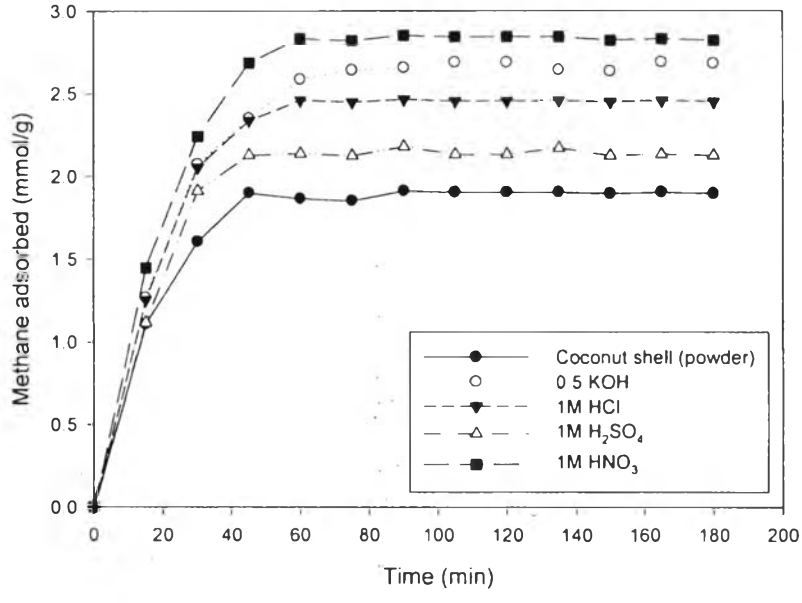

Figure 4.14 Methane uptake of activated carbons derived from coconut shell (powder) at 40°C temperature and 700 psi pressure.

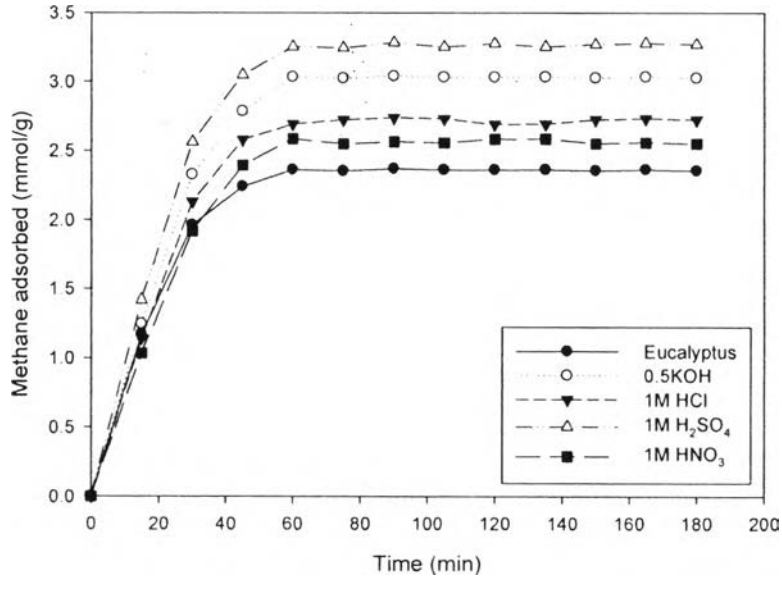

Figure 4.15 Methane uptake of activated carbons derived from eucalyptus at 40°C temperature and 700 psi pressure.

4.2.1 Methane Adsorption Isotherm

Adsorption isotherm was investigated at 40°C temperature and up to 700 psi pressure of methane. After applying methane pressure into reactor at each step, the system was leaved for 2 hours to reach adsorption equilibrium. Figure 4.17 to 4.21 show methane adsorption isotherm of activated carbon from Norit, from Calgon, from coconut shell (powder and 20-40 mesh) and from eucalyptus respectively. The adsorption isotherms were plotted by mole of methane adsorbed versus equilibrium pressure and by grams of methane adsorbed versus equilibrium pressure.

The adsorption isotherm results of all samples show in agreement with surface area result. The decreasing and increasing in surface area of adsorbents have effect on methane adsorption capacity. Wang *et al.* (2011) indicated that the higher surface area of activated carbon sample lead to higher amount of adsorption. The result from this experiment also shows the agreement with literature. The surface area of activated carbon has a significant effect on methane adsorption. In addition, Ahmadpour *et al.* (1998) inform that the raw material of carbons can effect on decreasing or increasing of surface area because of the different in composition.

As pointed out before, Xiao *et al.* (2008) and Santiago *et al.* (2005) refer that the impurities in pores are removed by the acid solution, leaving more pores to hold methane molecules. Simultaneously, the decrease in surface area due to remaining element and oxygenated terminal groups can make activated carbon becomes much harder to adsorb the molecules on their pore wall. In this experiment, the lower surface area of acid treated activated carbon from Norit and Calgon can adsorb less methane on their surface compared to the untreated. On the other hand, Xiao *et al.* (2007) indicated that the removal of impurities and increase in surface area and porosity after H_2SO_4 and HNO_3 treatment might improve methane storage capacity. Due to the impurities removal, the acid treated activated carbon derived from coconut shell and from eucalyptus show the higher surface area and the greater methane adsorption capacity also.

For base treatment, only the treated activated carbon from Norit show lower surface area than the untreated. Because of the lower surface area, activated carbon from Norit can adsorb less methane on their surface. According to

previous study (Sricharoenchaikul *et al.* (2007) and Ahmadpour *et al.* (1998), KOH can remove metal and mineral substance from crystallite of activated carbon structure and can create micropore in carbon structure. Therefore, the base treated activated carbon from Calgon, from coconut shell and from eucalyptus show the higher methane adsorption capacity than the untreated due to the oxidation reaction as in acid treatment.

Ahmadpour *et al.* (1998) indicated that the pore size distribution of activated carbon is an important factor for application in specific process operations. The method of treatment and type of solution is another parameter that may influence the final pore size distribution. Furthermore, Lozano-Castello *et al.* (2002) and Wang *et al.* (2011) indicated that the optimum pore size for methane storage applications is approximately 1.1 nm. However, all treated activated carbon in this experiment indicate only a slightly change in average pore diameter. As a result, the methane adsorption capacity relate only to the changing in surface area.

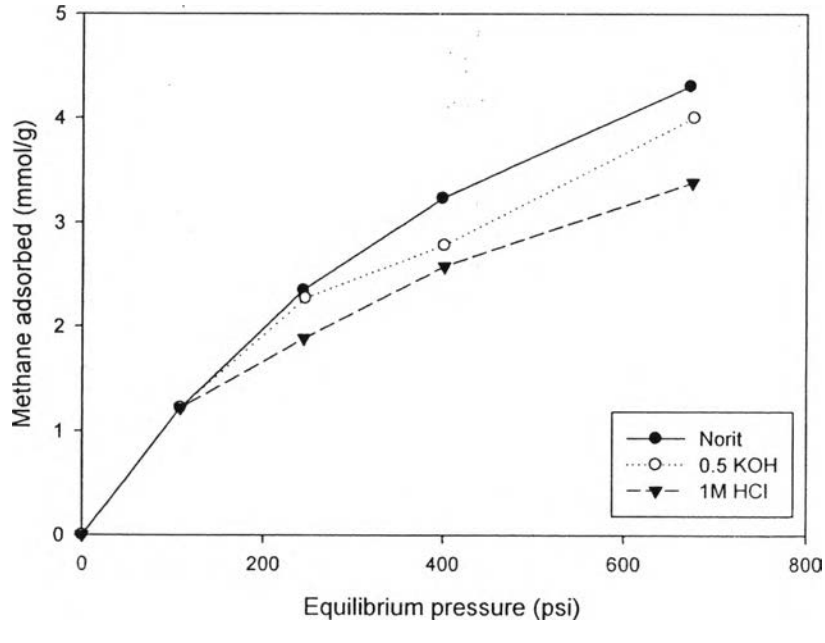

Figure 4.16 Adsorption isotherm of untreated and treated activated carbon from Norit.

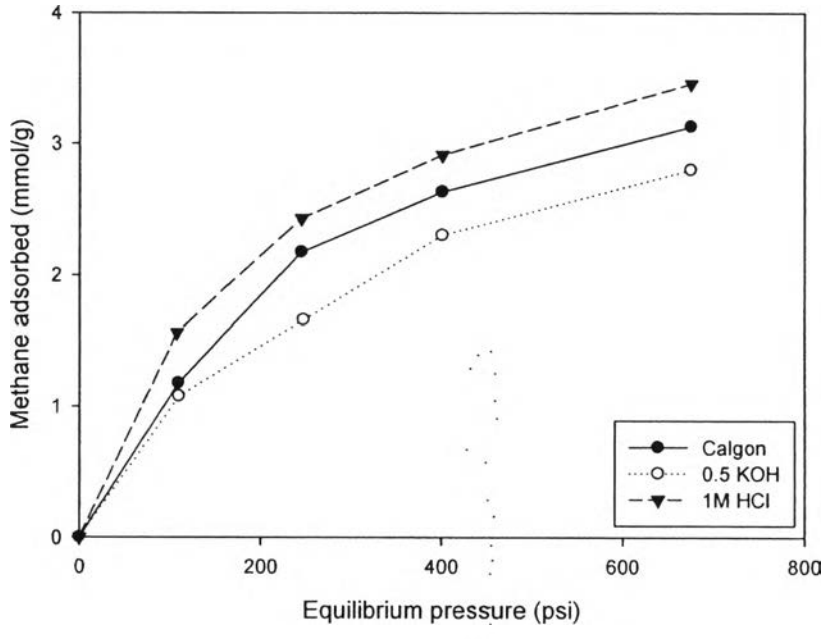

Figure 4.17 Adsorption isotherm of untreated and treated activated carbon from Calgon.

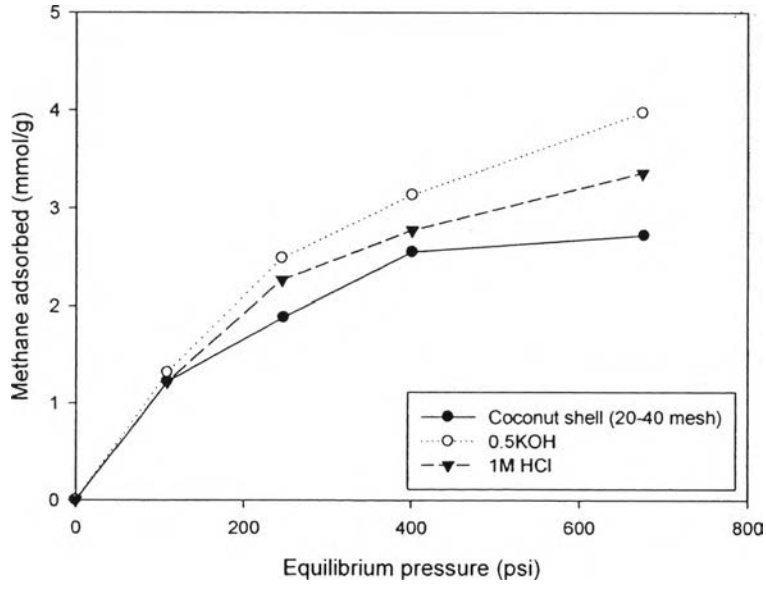

Figure 4.18 Adsorption isotherm of untreated and treated activated carbon derived from coconut shell (20-40 mesh).

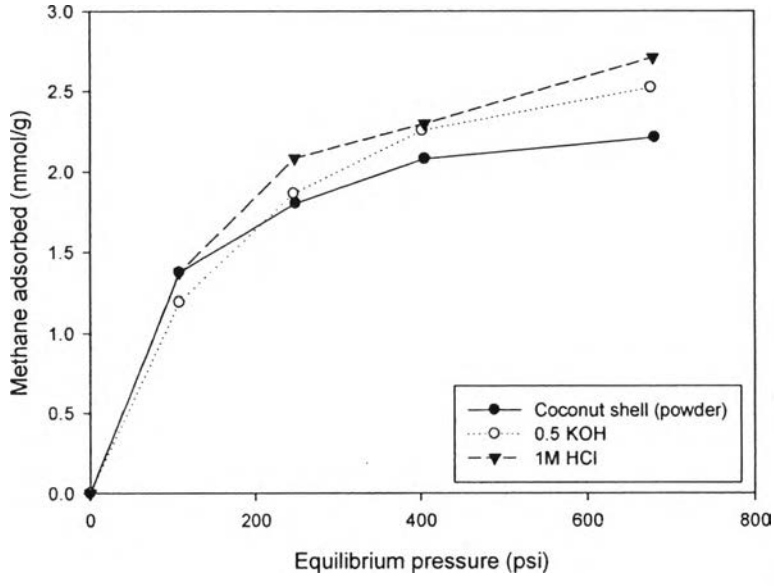

Figure 4.19 Adsorption isotherm of untreated and treated activated carbon derived from coconut shell (powder).

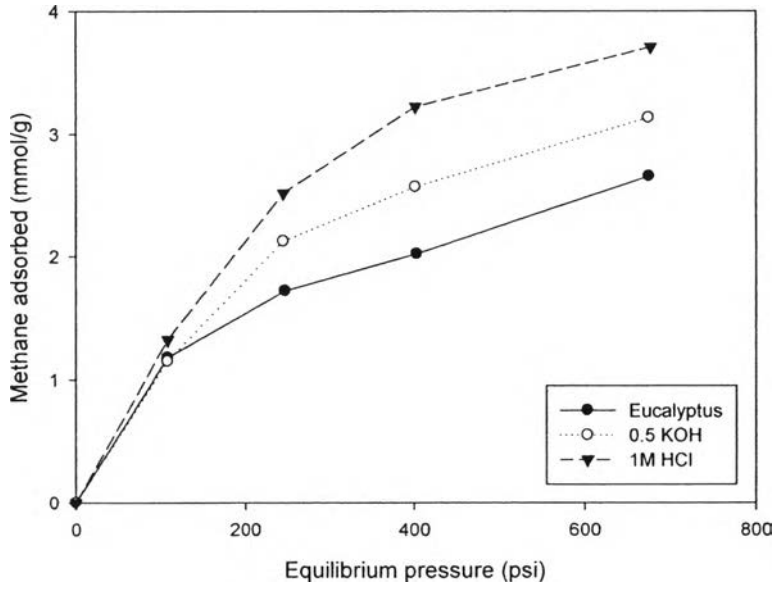

Figure 4.20 Adsorption isotherm of untreated and treated activated carbon derived from eucalyptus.

Another part of this experiment is treating all five activated carbon sample with liquid hydrocarbon to increase their hydrophobicity. Before applying the activated carbons into reactor, degassed carbon sample were mixed with 5%wt of decane. Figure 4.22 to 4.26 show the methane adsorption isotherm of treated and untreated activated carbons. The adsorption isotherms were plotted by mole of methane adsorbed versus equilibrium pressure and by grams of methane adsorbed versus equilibrium pressure.

At the lower methane pressure, all five of treated activated carbon can adsorb almost the same amount compared to the untreated. The 5%wt decane treated activated carbon sample from Norit show a slightly increasing of methane adsorption. On the other hand, the carbon from Calgon shows a small increasing of methane adsorption after mixing with decane. Almost the same amount of methane adsorbed as the untreated is observed from the activated carbon (20-40 mesh) that derived from coconut shell. On the treated activated carbon that derived from coconut shell (powder) and that derived from eucalyptus, the methane adsorption capacity is decreased after treatment. Although there are increasing and decreasing of amount of methane adsorbed after treatment, any conclusion cannot be drawn from these results. To determine effect of decane treatment on methane adsorption, further adsorption isotherm results are required. The adsorption isotherm at higher pressure or the adsorption isotherm of greater amount of decane added to the sample before apply into reactor should be done to investigate the decane treated activated carbon behavior.

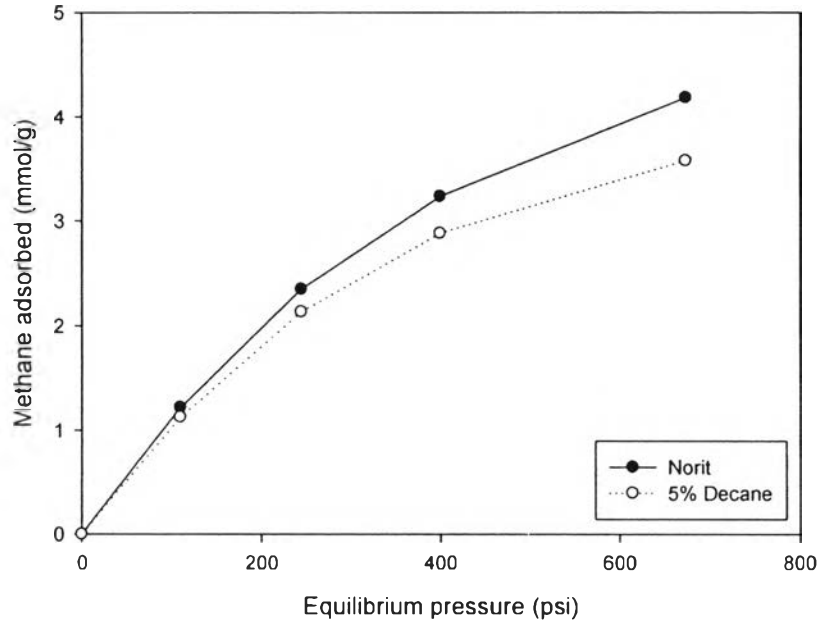

Figure 4.21 Adsorption isotherm of untreated and treated activated carbon from Norit.

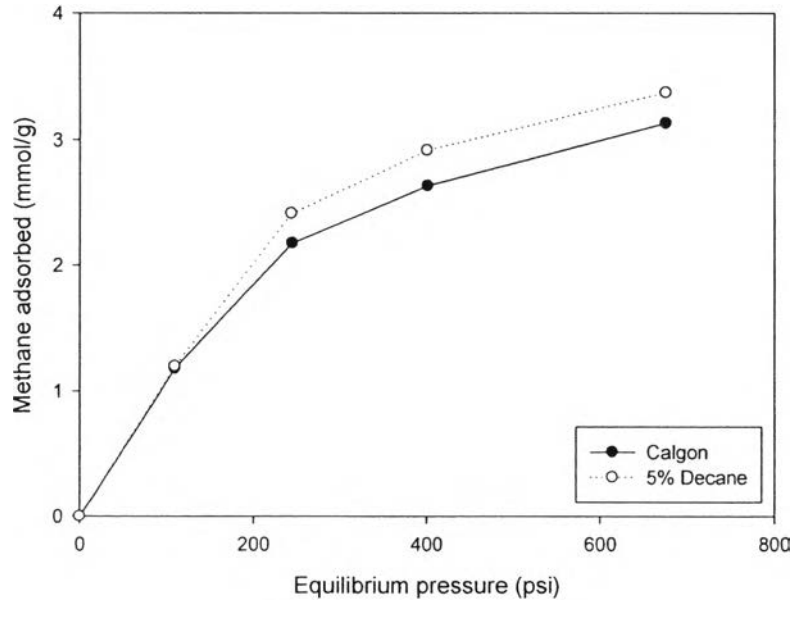

Figure 4.22 Adsorption isotherm of untreated and treated activated carbon from Calgon.

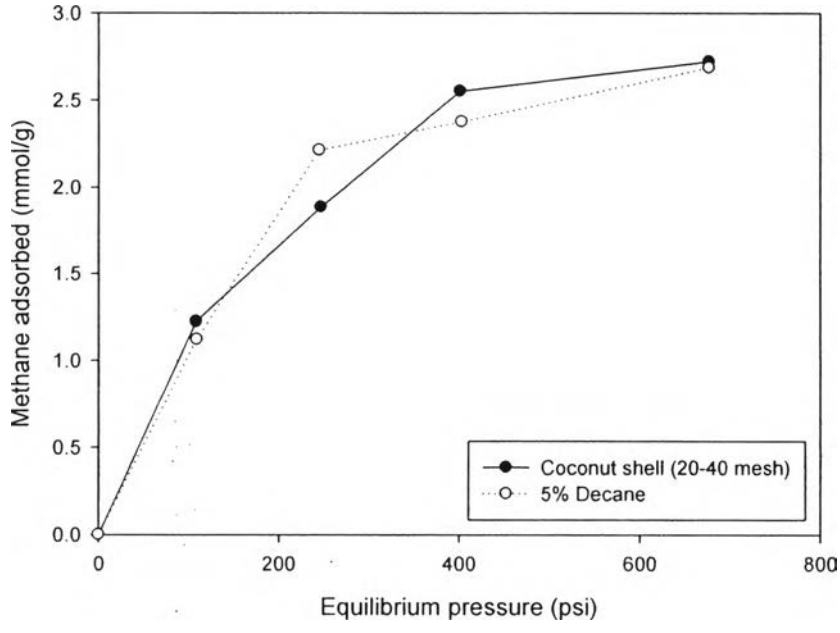

Figure 4.23 Adsorption isotherm of untreated and treated activated carbon derived from coconut shell (20-40 mesh).

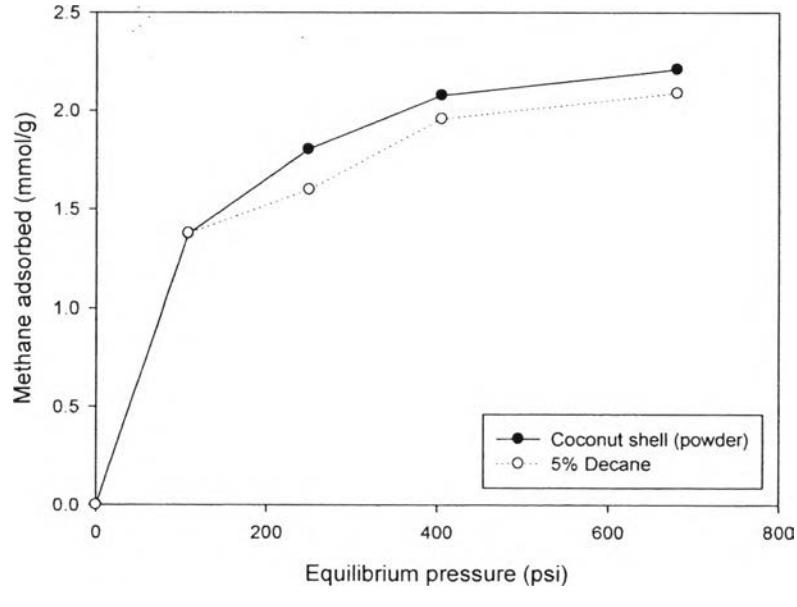

Figure 4.24 Adsorption isotherm of untreated and treated activated carbon derived from coconut shell (powder).

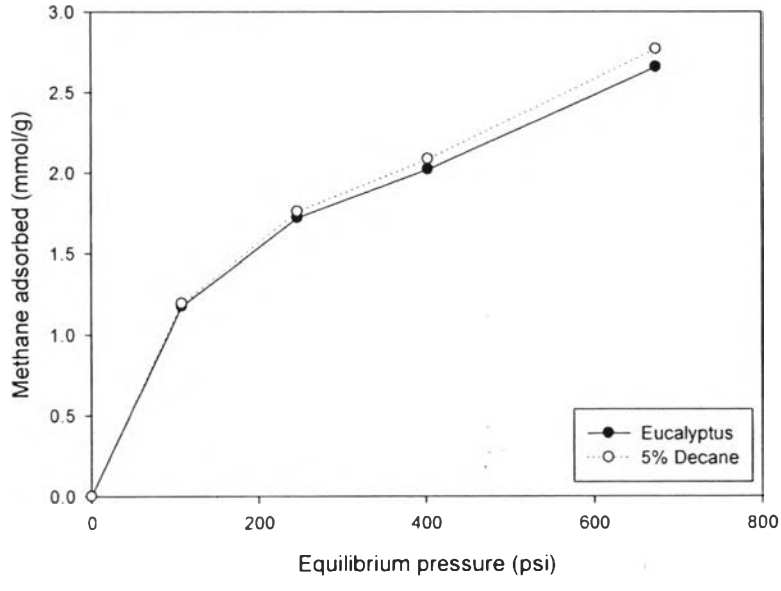

Figure 4.25 Adsorption isotherm of untreated and treated activated carbon derived from eucalyptus.